

This is a repository copy of *Mechanisms behind surface modification of polypropylene film using an atmospheric-pressure plasma jet*.

White Rose Research Online URL for this paper:

<https://eprints.whiterose.ac.uk/107107/>

Version: Accepted Version

Article:

Shaw, David orcid.org/0000-0001-5542-0334, West, Andrew orcid.org/0000-0003-4553-8640, Bredin, Jerome et al. (1 more author) (2016) Mechanisms behind surface modification of polypropylene film using an atmospheric-pressure plasma jet. *Plasma sources science & technology*. 065018. ISSN 0963-0252

<https://doi.org/10.1088/0963-0252/25/6/065018>

Reuse

This article is distributed under the terms of the Creative Commons Attribution (CC BY) licence. This licence allows you to distribute, remix, tweak, and build upon the work, even commercially, as long as you credit the authors for the original work. More information and the full terms of the licence here:

<https://creativecommons.org/licenses/>

Takedown

If you consider content in White Rose Research Online to be in breach of UK law, please notify us by emailing eprints@whiterose.ac.uk including the URL of the record and the reason for the withdrawal request.

Mechanisms behind surface modification of polypropylene film using an atmospheric-pressure plasma jet

David Shaw

York Plasma Institute, Department of Physics, University of York, York, YO10 5DD, UK

E-mail: drs518@york.ac.uk

Andrew West

York Plasma Institute, Department of Physics, University of York, York, YO10 5DD, UK

E-mail: andrew.west@york.ac.uk

Jerome Bredin

York Plasma Institute, Department of Physics, University of York, York, YO10 5DD, UK

E-mail: jerome.bredin@york.ac.uk

Erik Wagenaars

York Plasma Institute, Department of Physics, University of York, York, YO10 5DD, UK

E-mail: erik.wagenaars@york.ac.uk

Abstract. Plasma treatments are common for increasing the surface energy of plastics, such as polypropylene (PP), to create improved adhesive properties. Despite the significant differences in plasma sources and plasma properties used, similar effects on the plastic film can be achieved, suggesting a common dominant plasma constituent and underpinning mechanism. However, many details of this process are still unknown. Here we present a study into the mechanisms underpinning surface energy increase of PP using atmospheric-pressure plasmas. For this we use the effluent of an atmospheric-pressure plasma jet (APPJ) since, unlike most plasma sources used for these treatments, there is no direct contact between the plasma and the PP surface; the APPJ provides a neutral, radical-rich environment without charged particles and electric fields impinging on the PP surface. The APPJ is a RF-driven plasma operating in helium gas with small admixtures of O₂ (0-1 %), where the effluent propagates through open air towards the PP surface. Despite the lack of charged particles and electric fields on the PP surface, measurements of contact angle show a decrease from 93.9° to 70.1° in 1.4 s and to 35° in 120 s, corresponding to a rapid increase in surface energy from 36.4 mN/m to 66.5 mN/m in the short time of 1.4 s. These treatment effects are very similar to what is found in other devices, highlighting the importance of

Mechanisms behind surface modification of polypropylene film using an APPJ 2

neutral radicals produced by the plasma. Furthermore, we find an optimum percentage of oxygen of 0.5 % within the helium input gas, and a decrease of the treatment effect with distance between the APPJ and the PP surface. These observed effects are linked to two-photon absorption laser-induced fluorescence spectroscopy (TALIF) measurements of atomic oxygen density within the APPJ effluent which show similar trends, implying the importance of this radical in the surface treatment of PP. Analysis of the surface reveals a two stage mechanism for the production of polar bonds on the surface of the polymer: a fast reaction producing carboxylic acid, or a similar ketone, followed by a slower reaction that includes nitrogen from the atmosphere on the surface, producing amides from the ketones.

1. Introduction

Polypropylene (PP) is a thermoplastic with good heat, fatigue, and chemical resistance. It also remains translucent while being semi-rigid. This makes it very useful in applications such as food containment, textiles, packaging, and surgical implants [1]. The drawback, for some manufacturers that wish to adhere inks or glues to the polymer surface, is that these polymers have low wettability. To combat this; the industries involved are operating non-thermal plasmas to improve the polymers surface properties and allow for better adhesion or biocompatibility [2,3]. The plasma treatment only has an effect on the surface, and thus does not change the useful bulk properties of the material.

Over the years, many different plasma sources, operated under a range of conditions, have been used for surface modification of polymer films. Despite the significant differences that exist between these plasma sources, and more importantly their plasma properties, similar treatment effects can be achieved in terms of change in wettability. It has been suggested that the reason why polymer films have such low adhesion is due to a lack of surface polar groups [4]. So the plasmas increase the surface energy by either breaking polar bonds and leaving polar end groups, or by adding polar groups to the surface. This is an established general concept, however, there has been very little work that has linked the properties of the plasma with surface energy changes. Therefore, details on how the plasma breaks and adds bonds on the polymer surface are largely unknown, making optimisation of the plasma device an empirical and time-consuming process. Traditionally there have been low pressure treatments [5–8], but more recently there has been a focus on atmospheric pressure devices such as dielectric barrier discharge [9–12], coronal discharge [13], atmospheric glow discharge [14], or APPJs [15–20]. It is worth noting that all of this work has been done with devices where the plasma is in contact with the polymer surface. In this paper we aim to study the mechanisms underpinning the modification of PP surface using atmospheric-pressure plasmas. For this we reduce the complexity of the plasma that is treating the sample by using the effluent of a cross-field APPJ device. Here, there is no direct contact between the active plasma and the PP surface. Only the neutral radical-rich effluent reaches

the polymer, there are no charged particles or electric fields impinging on the surface. We are therefore able to isolate effects on the PP surface arising from radical species, excluding ion bombardment, charging and electric field effects.

2. Methods

2.1. Treatment of polypropylene films

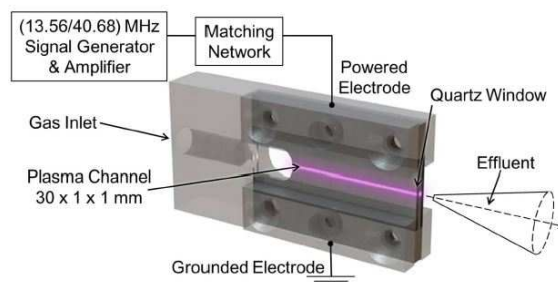


Figure 1. Schematic diagram of the Atmospheric-Pressure Plasma Jet (APPJ) used for this work

The plasma device used in this investigation was an atmospheric-pressure plasma jet (APPJ) shown in figure 1. It consists of two stainless steel electrodes and two quartz glass plates that form a 1 x 1 x 30 mm channel. A mixture of helium at 1 standard litre per minute, and oxygen at varying admixture percentages from 0.2 % up to 1 %, flows down the channel. One of the electrodes is driven via a matching network with radio frequency voltage of 13.56 MHz. The other electrode is grounded and plasma is formed across the channel. It is worth noting that the electric field created between the electrodes is perpendicular to the gas flow, meaning there are no significant electric fields present in the effluent of the APPJ. When the plasma leaves the end of the device and enters into open air it recombines very close to the nozzle due to the highly collisional environment at atmospheric pressure and the cross-field arrangement of the driving electric field. This leaves only a neutral, radical rich effluent for the surface treatments. For our experiments the APPJ is mounted on three axis motorised stages (Zaber T-LSM050A), and is pointed vertically downwards towards a polymer sample causing the effluent to impinge on the surface. Along with the O₂ percentage, the distance between the exit of the APPJ and the sample surface was varied, as was treatment time. The input power from the generator was kept constant at 30 W_{net}, though with losses through the matching network, the power dissipated in the plasma is much smaller, in the order of a few Watts.

The polymer films used throughout this investigation were PP with a thickness of 100 μm (Goodfellow Cambridge Ltd). A jig was constructed to hold the polymer beneath the APPJ for consistent location of treatment. For short treatment times (<

1
2
3 *Mechanisms behind surface modification of polypropylene film using an APPJ* 4

4
5 2 s) the APPJ was scanned along the surface at a calculated constant speed using the
6
7
8
9
10
11
12
13
14
15
16
17
18
19
20
21
22
23
24
25
26
27
28
29
30
31
32
33
34
35
36
37
38
39
40
41
42
43
44
45
46
47
48
49
50
51
52
53
54
55
56
57
58
59
60

the aforementioned motorised axial stages.

The density of atomic oxygen in the APPJ effluent was measured using two-photon absorption laser-induced fluorescence (TALIF) spectroscopy. The atomic oxygen TALIF scheme used for the measurements is discussed in detail by Niemi et al. [21] In short, two UV-photons at 225.65 nm are simultaneously absorbed to excite oxygen atoms from the $2p^4\ ^3P_2$ ground state into the $3p\ ^3P_{1,2,0}$ excited state. This subsequently decays, partially through optical transitions to the $3s\ ^3S$ state by emitting a near-infrared photon at 844.87 nm as described by Niemi et al. and Knake et al. [22] The effective collisional-induced quenching rate is estimated using radiative lifetimes and quenching coefficients from [21], assuming the feedstock gases are the sole quenching partners at 300 Kelvin. This provides estimates of relative ground state atomic oxygen density.

2.2. Surface characterisation

The surface modification was monitored using a contact angle analyser (Dyne Technology, Theta Lite) which measures changes in wettability through the static sessile drop method. It consists of a camera that looks across the treated surface, and a needled syringe that creates controlled volume droplets which are placed onto the surface from above. The camera records images of the droplet which are used to calculate the contact angle between the liquid and the treated surface. Each recorded droplet consisted of 24 individual images which were individually analysed for their contact angles. An average result was obtained per droplet with the standard deviation. Each treatment was repeated and analysed a minimum of three times and weighted mean was calculated. The standard deviation of the mean is given as the error and is propagated through further calculations. Two liquids were used; deionised water, and diiodomethane (Sigma-Aldrich). The calculation of the surface energy was performed using the Owens-Wendt-Rabel-Kaelble (OWRK) method [23]. This method uses the difference between the polar and dispersive components of the two liquids. All liquids have a dispersive component, deionised water is a polar liquid and thus it also has available polar bonds. Diiodomethane is non-polar and thus has no available polar bonds. The dispersive component is mechanical and based around the van der Waals force. The polar component is chemical and reveals polar end bonds available for the liquid on the surface. This allows us to characterise whether the changes in contact angle being seen are due to a mechanical roughening, or a molecular scale chemical reaction on the surface.

To analyse the chemistry on the surface Attenuated Total Reflectance Fourier Transform Infrared spectroscopy (ATR-FTIR, Thermo Scientific Nicolet iS50) was used. The sample is mounted on a diamond holder and a beam of IR light is totally internally reflected within the crystal. An evanescent wave extends beyond the interface and into the sample and is attenuated by regions that absorb the energy of the wave. This is then passed into the internally reflected beam and on to an IR spectrometer for analysis.

3. Results

3.1. APPJ operational parameter variations

In order to investigate the underpinning physics of the APPJ treatment of a PP surface, we measured contact angle while varying three operational parameters of the APPJ, oxygen admixture, treatment time, and distance.

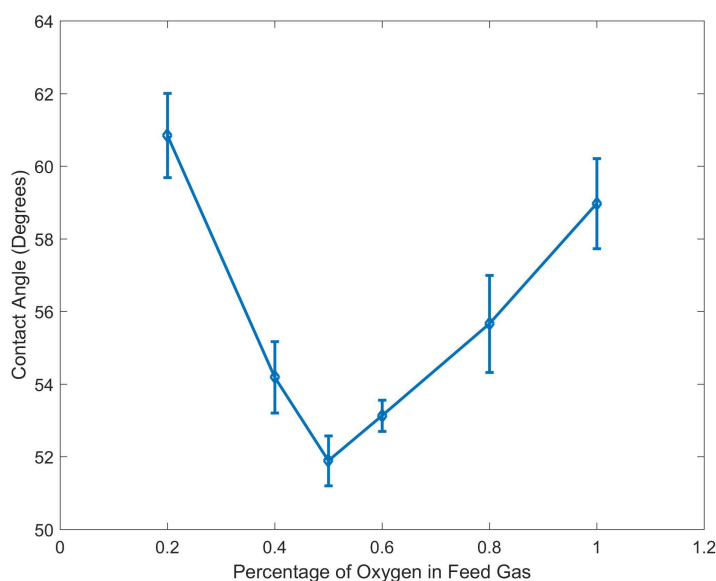


Figure 2. Contact angle changes as a function of percentage of O_2 admixture in the feed gas after 30 seconds of treatment time. The untreated PP was measured to have a contact angle of 93.9°

When varying the oxygen admixture in the feed gas the APPJ was placed at 15 mm above the sample surface. Figure 2 shows the measured contact angle after the treatment for various oxygen admixtures. For all admixtures there is a significant reduction in contact angle compared to the untreated PP, which has a contact angle of 93.9° . Despite the fact that our plasma jet only provides neutral radicals and no charged particles or electric fields, we observe changes in contact angle from 93.9° to 51.9° in 30 s. This is similar to other APPJ treatments such as the 52.0° achieved by Kostov [16]. Nevertheless, there is a clear difference in the treatment effect with the largest change in contact angle, after 30 seconds of treatment time, with 0.5 % oxygen. Increasing the oxygen percentage above 0.5 % leads to a reduced effect of the treatment.

Figure 3 shows the measured contact angle as a function of treatment time while keeping the distance and oxygen percentage constant. It is clear that there is a very rapid decrease in contact angle during the first 10 seconds, with a further, much slower reduction in contact angle between 20 and 120 seconds. The decreasing trend suggests that a further reduction can be expected for treatment times beyond 120 sec. To investigate the initial, sharp decrease in contact angle further, we performed plasma

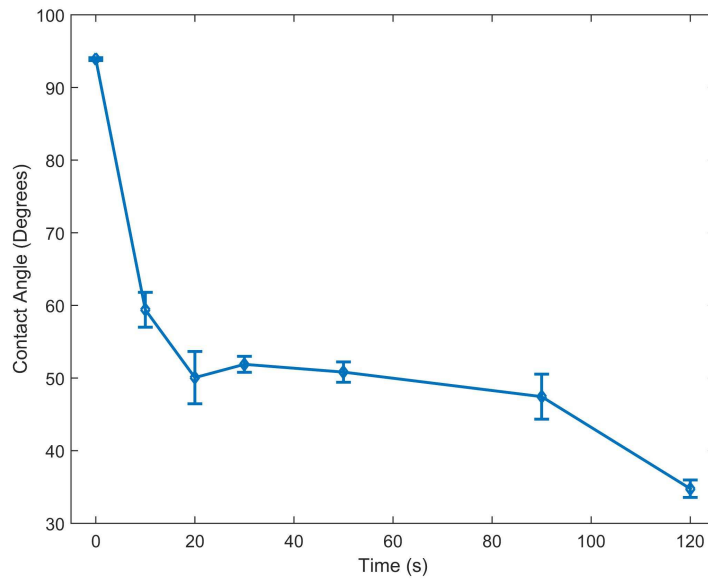


Figure 3. Contact angle changes with APPJ treatment time for PP with 0.5 % O₂ in the feed gas and a distance of 15 mm

treatments between 0.2 and 2 seconds as shown in figure 4. Here we observe a very fast drop in contact angle from 93.9 ° to 70.1 ° in only 1.5 seconds. This means 40 % of the total contact angle reduction happens in the first 1.5 seconds. It seems that there are two processes at play that both result in a reduction of contact angle. One is fast, reaching its maximum effect after 1.5 sec, while the second is much slower but continues for at least 120 seconds.

The final operational parameter that was investigated was the distance between the nozzle of the APPJ and the surface of the PP film. The O₂ admixture was kept at the optimum of 0.5 %, while for various distances we recorded the treatment effect as function of time. The results are shown in figure 5. For short distances, 3 to 15 mm, we again observe a two-stage decrease in contact angle, a rapid decrease < 10 seconds and a more gradual, continuing decrease 20 - 120 seconds. For larger distances 30 and 50 mm, there appears to only be the slow, gradual decrease. It is interesting to note that all distances below 15 mm have a very similar effect for each treatment time while for distances larger than 15 mm there is a clear decrease in effect for increasing distance at any given treatment time.

3.2. Surface energy

Using the aforementioned OWRK method it is possible to use contact angle measurements to calculate surface energy and split it into its two component parts. Taking contact angle measurements for the original 0.5 % O₂ admixture with diiodomethane showed a similar drop in contact angle with treatment time to that of water. However, when the OWRK method is used, the polar and dispersive elements

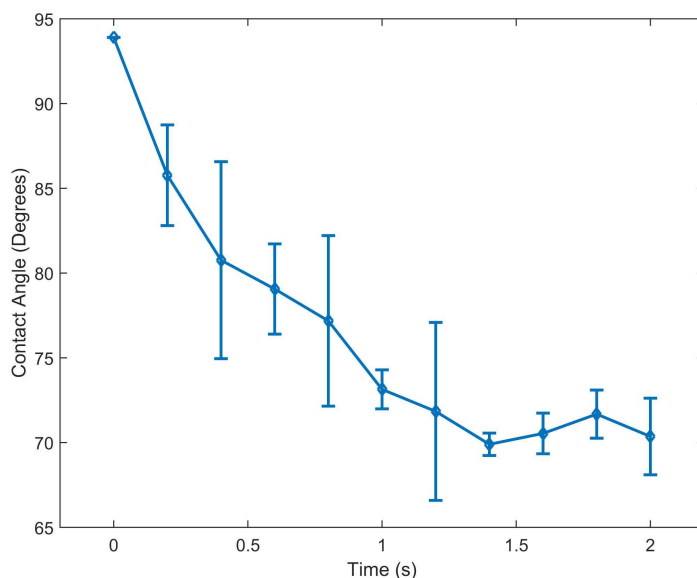


Figure 4. Contact angle changes with short APPJ treatment time for PP with 0.5 % O_2 in the feed gas and a distance of 15 mm between the APPJ and the PP surface

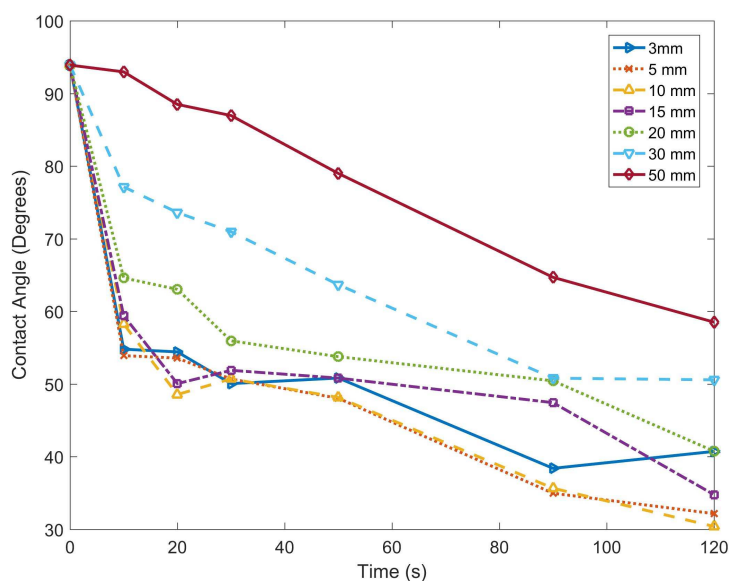


Figure 5. Contact angle changes with APPJ treatment time and distance. Errors are not included for clarity but are similar to those presented in previous figures

of the surface energy of the PP are revealed. These results are shown in figure 6. There is a total increase in surface energy that matches the drop in contact angle previously shown in figure 3. The dispersive component appears invariant in time, with a value of around 30 mN/m, whereas the polar component shows an increase in energy from 10 mN/m to 55 mN/m after 30 seconds of treatment.

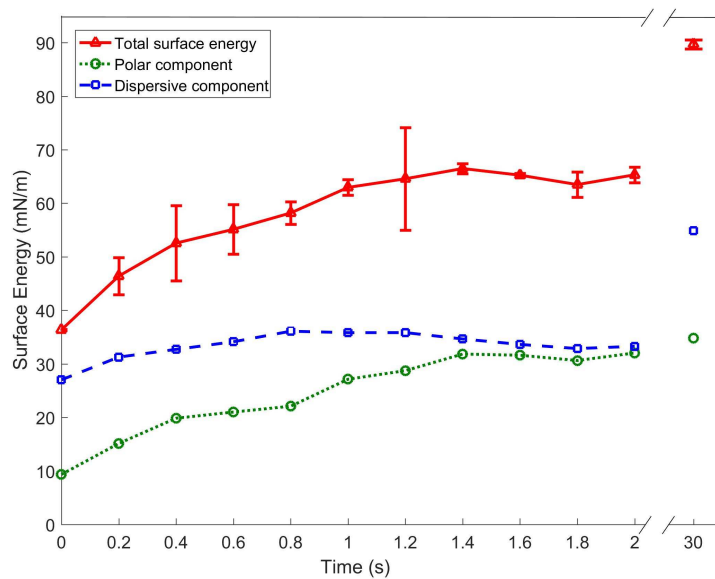


Figure 6. Surface energy of PP treated with an APPJ at 15 mm with 30 W_{net} power and 0.5 % O_2 admixture in the He feed gas. Errors are shown only for the total surface energy for clarity as they are propagated from original measurements

3.3. Surface analysis

The ATR-FTIR measurements of the surface showed an area of interest between wavenumbers 1500 and 1900 cm^{-1} shown in Figure 7. These could be absorption of water, however there is no corresponding peak in the data between 3000 and 4000 wavenumbers making this unlikely. Thus this area shows carbonyl stretching bands being formed on the surface of the PP. The increase in absorption with treatment time is due to a carbon oxygen double bond ($C=O$), the details of which depend on the exact location of the dip [24]. The large dip on the 2 min treatment time at about 1720 cm^{-1} , that does not exist in the untreated spectrum, could be due to one of two possibilities. Either it is carboxylic acid ($RC(=O)OH$), or it is another similar ketone (an organic compound with a structure $RC(=O)R'$) [25]. The dip around 1650 cm^{-1} can be attributed to conjugated ketones, which are similar to regular ketones apart from the alternating double and single bonds that allow for more freedom of movement of electrons. Another dip grows through treatment at 1670 cm^{-1} which is most likely an increase in the amide functional group. Amides can be produced from carboxylic acids, but do involve the inclusion of a nitrogen atom [26]. It is important to note, for comparison between this atmospheric method and low-pressure methods, that the increase in the amide functional group can only be achieved with the inclusion of nitrogen. This has only been possible in this work due to the nitrogen in the atmosphere.

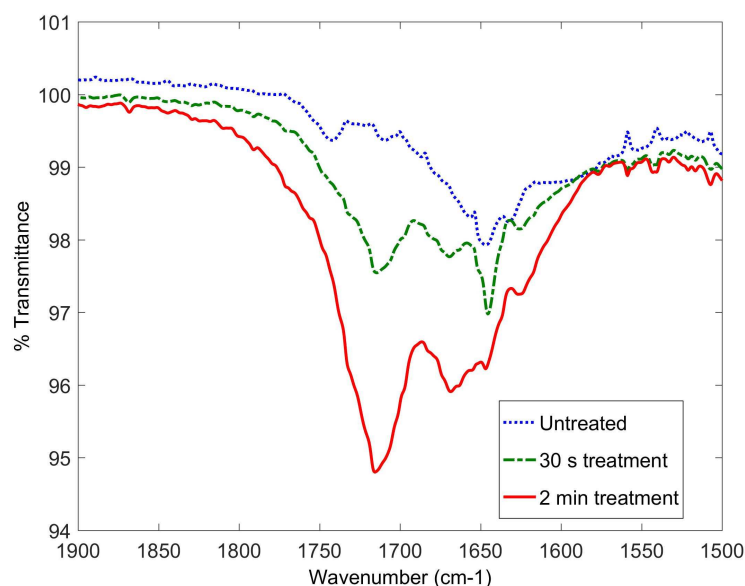


Figure 7. ATR-FTIR spectrum of PP before and after treatment at 15 mm, 0.5 % O₂ in the He feed gas, and an input power of 30 W_{net}

3.4. Surface modification pathways

From these measurements we attempt to obtain insight into the reaction pathways of the surface modification. The FTIR measurements show the well-known and well understood signs of oxidation of the PP, this suggests oxygen species from the plasma are dominant in observed modifications. However, the plasma chemistry of APPJs is well characterised and there are several reactive oxygen species produced, e.g. atomic oxygen, singlet delta oxygen, and ozone. We performed TALIF experiments to measure the atomic oxygen densities at the exit of the APPJ as a function of oxygen admixture. The results in figure 8 show a strong correlation with the observed changes in contact angle. I.e. a maximum treatment effect at 0.5 % oxygen, when the concentration of O is maximum. The TALIF measurements agree with the O density measurements done by Knake [22]. Other reactive oxygen species have been measured in the same device. Sousa et al measured singlet delta oxygen [27], and Ellerweg et al ozone [28]. Singlet delta oxygen was shown to decrease with increasing oxygen admixture between 0.1 % and 0.7 %, and ozone was shown to increase over the same range. Furthermore, it is known that the density of atomic oxygen decreases exponentially with increased distance from the APPJ nozzle [21, 22], whereas ozone is a long-lived radical species. All of this suggests a direct link between the production of atomic oxygen in the APPJ and the observed modification of the PP surface.

The results in figure 5 suggest that the observed fast change in contact angle is dependent on the number of reactive species at the PP surface, i.e. for large distances, the radical density is lower and therefore the observed effect is less. The slow change that is observed for all distances appears to depend on flux to the surface. The same change

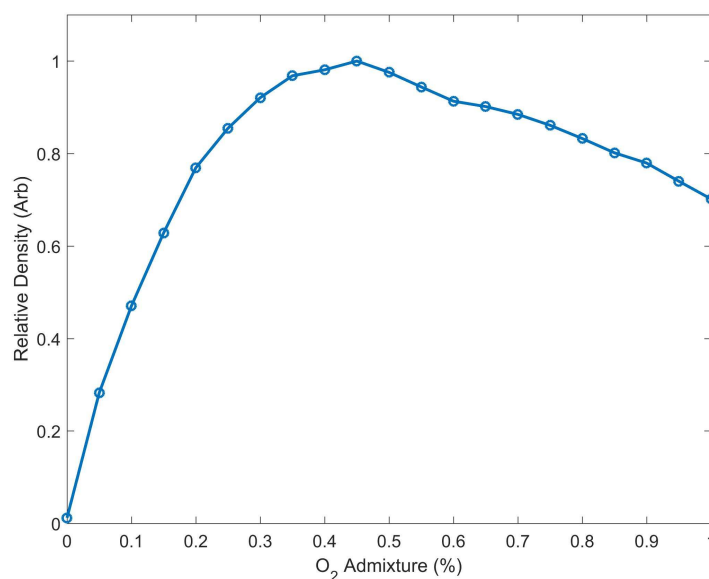


Figure 8. TALIF measurement of the relative densities of atomic oxygen in the effluent of the APPJ as a function of O₂ percentage in the input gas.

in contact angle can be achieved for larger distances (smaller radical concentrations) by increasing the treatment time, resulting in similar fluxes. The pathways linked to the two observed surface processes can be explained with the FTIR measurements. The initial reaction shows production of carboxylic acid, or a similar ketone, and some conjugated ketones. The pathways of which are well understood [29]. This is a fast reaction that takes depends highly on the density of the atomic oxygen reaching the surface. The slow reaction is in part due to the inclusion of the nitrogen in the atmosphere which produces amides from the ketones created by the atomic oxygen. In addition ozone could also be involved within the slow reaction at the longer distances. It is clear that in both the fast and slow processes atomic oxygen from the APPJ plays a key role.

4. Conclusion

Using the radical-only effluent of an APPJ we were able to induce rapid and large increases in surface energy of PP films; a decrease in contact angle from 93.9 ° to 70.1 ° in 1.4 s and to 35 ° in 120 s, corresponding to an increase in surface energy from 36.4 mN/m to 66.5 mN/m in 1.4 s. These treatment effects are similar in scale to what is achieved with other devices, highlighting the importance of neutral radicals in plasma-induced PP modification. Further investigations using TALIF identify atomic oxygen as the dominant radical in these treatments. Unlike other radicals such as singlet delta oxygen and ozone, the measured O densities as a function of oxygen admixture match the observed changes in surface energy. Finally, FTIR surface analysis reveals a two stage mechanism for the production of polar bonds on the PP surface: A fast reaction

producing carboxylic acid, or a similar ketone. Followed by a slower reaction which is likely to be a combination of ozone producing ketones, and nitrogen forming amides from the ketones.

References

- [1] J. F. Friedrich, L. Wigant, W. Unger, A. Lippitz, H. Wittrich, D. Prescher, J. Erdmann, H. V. Gorsler, and L. Nick. Barrier properties of plasma-modified polypropylene and polyethyleneterephthalate. *J. Adhes. Sci. Technol.*, 9(9):1165, **1995**. URL <http://www.scopus.com/inward/record.url?eid=2-s2.0-0029192603&partnerID=tZ0tx3y1>.
- [2] C.-m. Chan. *Polymer Surface Modification and Characterization*. Carl Hanser, GmbH & Co., New York, **1994**.
- [3] A. Kuzminova, M. Vandrovcová, A. Shelemin, O. Kylián, A. Choukourov, J. Hanuš, L. Bačáková, D. Slavínská, and H. Biederman. Treatment of poly(ethylene terephthalate) foils by atmospheric pressure air dielectric barrier discharge and its influence on cell growth. *Appl. Surf. Sci.*, 357:689, **2015**. URL <http://linkinghub.elsevier.com/retrieve/pii/S0169433215021765>.
- [4] A. Salimi. Characterization of nano scale adhesion at solid surface of oxidized PP wax/PP blends. *Int. J. Adhes. Adhes.*, 33:61, **2012**. URL <http://dx.doi.org/10.1016/j.ijadhadh.2011.11.004>.
- [5] C. Muhlhan, S. Weidner, J. Friedrich, and H. Nowack. Improvement of bonding properties of polypropylene by low- pressure plasma treatment. *Surf. Coatings Technol.*, 119:783, **1999**.
- [6] D. Hegemann, H. Brunner, and C. Oehr. Plasma treatment of polymers for surface and adhesion improvement. *Nucl. Instruments Methods Phys. Res. Sect. B Beam Interact. with Mater. Atoms*, 208:281, **2003**. URL <http://linkinghub.elsevier.com/retrieve/pii/S0168583X0300644X>.
- [7] N. Shahidzadeh-Ahmadi, M. Chehimi, F. Arefi-Khonsari, N. Foulon-Belkacemi, J. Amouroux, and M. Delamar. A physicochemical study of oxygen plasma-modified polypropylene. *Colloids Surfaces A Physicochem. Eng. Asp.*, 105(2-3):277, **1995**. URL <http://linkinghub.elsevier.com/retrieve/pii/S0927775795033149>.
- [8] K. N. Pandiyaraj, V. Selvarajan, R. Deshmukh, and C. Gao. Modification of surface properties of polypropylene (PP) film using DC glow discharge air plasma. *Appl. Surf. Sci.*, 255(7):3965, **2009**. URL <http://www.sciencedirect.com/science/article/pii/S0169433208022101>.
- [9] K. G. Kostov, T. M. C. Nishime, L. R. O. Hein, and a. Toth. Study of polypropylene surface modification by air dielectric barrier discharge operated at two different frequencies. *Surf. Coatings Technol.*, 234:60, **2013**. URL <http://dx.doi.org/10.1016/j.surfcoat.2012.09.041>.
- [10] N. De Geyter, R. Morent, C. Leys, L. Gengembre, and E. Payen. Treatment of polymer films with a dielectric barrier discharge in air, helium and argon at medium pressure. *Surf. Coatings Technol.*, 201(16-17):7066, **2007**.
- [11] F. Massines and G. Gouda. A comparison of polypropylene-surface treatment by filamentary, homogeneous and glow discharges in helium at atmospheric pressure. *J. Phys. D. Appl. Phys.*, 31:3411, **1999**.
- [12] N.-Y. Cui and N. M. Brown. Modification of the surface properties of a polypropylene (PP) film using an air dielectric barrier discharge plasma. *Appl. Surf. Sci.*, 189(1-2):31, **2002**. URL <http://www.sciencedirect.com/science/article/pii/S0169433201010352>.
- [13] M. Zenkiewicz. Investigation on the oxidation of surface layers of polyolefins treated with corona discharge. *J. Adhes. Sci. Technol.*, 15(1):63, **2001**. URL <http://www.tandfonline.com/doi/abs/10.1163/156856101743319>.
- [14] A. C. Ruddy. The Effect of Atmospheric Glow Discharge (APGD) Treatment on Polyetherimide, Polybutyleneterephthalate, and Polyamides. *J. Plast. Film Sheeting*, 22(2):103, **2006**.
- [15] A. Van Deynse, P. Cools, C. Leys, N. De Geyter, and R. Morent. Surface activation of polyethylene

Mechanisms behind surface modification of polypropylene film using an APPJ 12

- with an argon atmospheric pressure plasma jet: Influence of applied power and flow rate. *Appl. Surf. Sci.*, 328:269, **2015**. URL <http://linkinghub.elsevier.com/retrieve/pii/S0169433214027639>.
- [16] K. Kostov, T. Nishime, A. Castro, A. Toth, and L. Hein. Surface modification of polymeric materials by cold atmospheric plasma jet. *Appl. Surf. Sci.*, 314(1-4):367, **2014**. URL <http://dx.doi.org/10.1016/j.apsusc.2014.07.009><http://linkinghub.elsevier.com/retrieve/pii/S0300944097001173><http://linkinghub.elsevier.com/retrieve/pii/S0169433214015232>.
- [17] J. A. Jofre-Reche, J. Pulpytel, H. Fakhouri, F. Arefi-Khonsari, and J. M. Martín-Martínez. Surface Treatment of Polydimethylsiloxane (PDMS) with Atmospheric Pressure Rotating Plasma Jet. Modeling and Optimization of the Surface Treatment Conditions. *Plasma Process. Polym.*, page DOI: 10.1002/ppap.201500118, **2015**. URL <http://doi.wiley.com/10.1002/ppap.201500118>.
- [18] J. Sun and Y. Qiu. The Effects of Gas Composition on the Atmospheric Pressure Plasma Jet Modification of Polyethylene Films. *Plasma Sci. Technol.*, 17(5):402, **2015**. URL <http://stacks.iop.org/1009-0630/17/i=5/a=402?key=crossref.9d2deb3fabc0b3670ff9145ad9d6a560>.
- [19] G.-L. Chen, X. Zheng, J. Huang, X.-L. Si, Z.-L. Chen, F. Xue, and S. Massey. Three different low-temperature plasma-based methods for hydrophilicity improvement of polyethylene films at atmospheric pressure. *Chinese Phys. B*, 22(11):115206, **2013**. URL <http://stacks.iop.org/1674-1056/22/i=11/a=115206?key=crossref.f1cbf90cadf67e516294117f6aa0f56f>.
- [20] U. Lommatzsch, D. Pasedag, A. Baalman, G. Ellinghorst, and H. E. Wagner. Atmospheric pressure plasma jet treatment of polyethylene surfaces for adhesion improvement. *Plasma Process. Polym.*, 4(SUPPL.1):1041, **2007**.
- [21] K. Niemi, V. S.-v. D. Gathen, and H. F. Dobe. Absolute atomic oxygen density measurements by two-photon absorption laser-induced fluorescence spectroscopy in an RF-excited atmospheric pressure plasma jet. *Plasma Sources Sci. Technol.*, 14(2):375, **2005**.
- [22] N. Knake, K. Niemi, S. Reuter, V. Schulz-von der Gathen, and J. Winter. Absolute atomic oxygen density profiles in the discharge core of a microscale atmospheric pressure plasma jet. *Appl. Phys. Lett.*, 93(13):131503, **2008**. URL <http://scitation.aip.org/content/aip/journal/apl/93/13/10.1063/1.2995983>.
- [23] D. K. Owens and R. C. Wendt. Estimation of the surface free energy of polymers. *J. Appl. Polym. Sci.*, 13(8):1741, **1969**. URL <http://doi.wiley.com/10.1002/app.1969.070130815>.
- [24] J. Coates. Interpretation of Infrared Spectra, A Practical Approach. *Encycl. Anal. Chem.*, pages 10,815–10,837, **2000**.
- [25] G. P. Moss, P. a. S. Smith, and D. Tavernier. Glossary of Class Names of Organic Compounds and Reactive Intermediates Based on Structure. *Pure Appl. Chem.*, 67:1307, **1995**.
- [26] J. Deruiter. Amides and related functional groups, **2005**. URL [http://www.auburn.edu/\\$\sim\\$sim\\$deruija/pda1_amides.pdf](http://www.auburn.edu/\simsim$deruija/pda1_amides.pdf).
- [27] J. S. Sousa, K. Niemi, L. J. Cox, Q. T. Algwari, T. Gans, D. O'Connell, and D. OConnell. Cold atmospheric pressure plasma jets as sources of singlet delta oxygen for biomedical applications. *J. Appl. Phys.*, 109(12):0, **2011**. URL <http://www.scopus.com/inward/record.url?eid=2-s2.0-79960166586&partnerID=tZ0tx3y1>.
- [28] D. Ellerweg, J. Benedikt, A. von Keudell, N. Knake, and V. Schulz-von der Gathen. Characterization of the effluent of a He/O₂ microscale atmospheric pressure plasma jet by quantitative molecular beam mass spectrometry. *New J. Phys.*, 12(1):013021, **2010**. URL <http://stacks.iop.org/1367-2630/12/i=1/a=013021?key=crossref.47f89e56b7d7485f578d052b7711abd2>.
- [29] R. Dorai and M. J. Kushner. A model for plasma modification of polypropylene using atmospheric pressure discharges. *J. Phys. D. Appl. Phys.*, 36(6):666, **2003**. URL <http://stacks.iop.org/0022-3727/36/i=6/a=309?key=crossref.033f56c3493687f25084617e1f8c29c8>.

1
2
3 *Mechanisms behind surface modification of polypropylene film using an APPJ* 13

4
5 *Acknowledgements*

6
7 This work was supported by the Engineering and Physical Sciences Research Council
8 (EPSRC) [EP/L01663X/1 & EP/K018388/1]
9
10
11
12
13
14
15
16
17
18
19
20
21
22
23
24
25
26
27
28
29
30
31
32
33
34
35
36
37
38
39
40
41
42
43
44
45
46
47
48
49
50
51
52
53
54
55
56
57
58
59
60